Coherent polarization beam combining of four polarization-maintained fiber amplifiers using single-frequency dithering technique

Pengfei Ma (马鹏飞), Pu Zhou (周 朴), Yanxing Ma (马阎星), Rongtao Su (粟荣涛), and Zejin Liu (刘泽金)*

College of Optoelectric Science and Engineering, National University of Defense Technology, Changsha 410073, China

**Corresponding author: zejinliu@vip.sina.com*

Received January 4, 2012; accepted February 24, 2012; posted online May 16, 2012

In this manuscript, coherent polarization beam combining of four polarization-maintained fiber amplifiers is demonstrated. In each fiber amplifier, two cascaded fiber amplification stages are used to boost the output power to watt level. The compact and robust single-frequency dithering technique is employed in the active phase-locking of the four laser beams. When the system is in the closed loop, the phase noise can be suppressed effectively for long-time observation. The experimental results show that the combining efficiency of the whole system is as high as 95%.

OCIS codes: 140.3280, 140.3290, 140.3580.

doi: 10.3788/COL201210.081404.

Fiber lasers and amplifiers have great potential in scaling to high power levels with diffraction-limited beam quality. However, several obstacles, including the limits on high brightness pump diodes, fiber damage, thermal effects and nonlinear effects, can ultimately limit the maximal output power[1−2]. Coherent beam combination (CBC) of several laser elements provides a feasible solution[3−13]. Most CBC structures incorporate multiple tiled emitters that induce a portion of power encircled into the sidelobes in the far-field pattern[14], which degrades the beam quality inevitably. As one of the CBC structures, coherent polarization beam combining (CPBC) eliminates the deficiency of sidelobes, because all the beams are coaxially combined in this technique. In this letter, we demonstrate the CPBC of four polarization-maintained fiber amplifiers. The system performs well in the closed loop, and the combining efficiency can reach 95%. It is noteworthy that the single-frequency dithering technique is employed. This technique is compact and effective compared with the heterodyne detection phase control technique reported in previous demonstrations[15,16].

The experimental configuration is shown in Fig. 1. The seed laser used was a single-frequency Yb-doped fiber laser with central wavelength of 1062.6 nm and a linewidth of less than 20 kHz using ultra-short laser cavity[17]. The laser power from the seed laser through the isolator (ISO) was about 60 mW. The seed laser was split into four channels and coupled to four phase modulators (PMs). The PMs used were $LiNbO_3$ phase modulators (Photline Technologies Corporation) with over 100-MHz modulating bandwidth working at a wavelength of 1060 nm. The output power from each phase modulators was more than 10 mW, the loss of laser power was induced by the insertion loss of the modulators. Then each fiber channel was coupled to a 2-stage all-fiber amplifier created by the authors of the present work. The active fiber in the first stage was a polarization-maintained single-clad Yb-doped fiber that had a core diameter of 6 μm and a cladding diameter of 125 μm. After pumping by a 200-mW single-mode fiber pigtailed laser diode with a 974-nm central wavelength, the laser power in each channel increased to over 100 mW. The active fiber in the second stage was a polarization-maintained double-clad Yb-doped fiber, which had a 10-μm core diameter and 125-μm inner cladding diameter. The numerical aperture (NA) values of the core and the inner cladding of the double-clad fiber were 0.075 and 0.46, respectively. The laser beam was strictly single mode because the double-clad fiber had a V number of 2.22 for 1060-nm laser operation. A multimode laser diode with 975-nm central wavelength, 105-μm pigtailed fiber, and a maximal output power of 3 W was used to pump the active double-clad fiber in each channel using a (2+1) ×1 pump combiner. The left unused pump port was used to monitor the backscattering light in the case of nonlinear effect due to the single-frequency amplification process. The active fiber in the second stage has an absorption coefficient of 5.5 dB/m at 975-nm pump wavelength. In each channel,

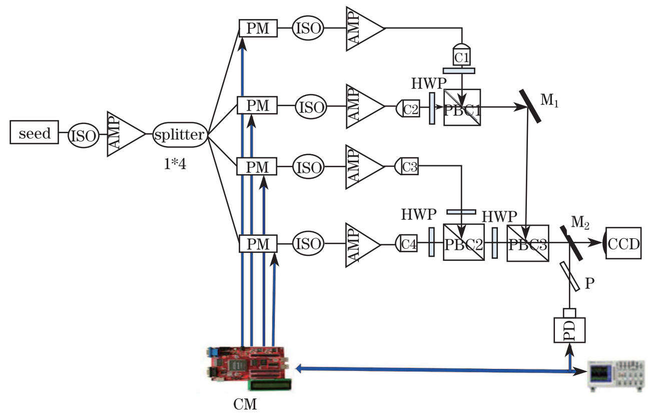

Fig. 1. Experimental setup of the CPBC of four fiber beams. C1-C4: collimator with embedded isolator; P: polarizer; PD: photo detector; AMP: cascaded two-stage amplifier.

an active fiber with a length of 4 m was employed. A section of passive fiber was spliced after the active fiber for output power delivery. The spliced region was covered in high-index gel to strip out the residual pump laser. Then, the passive fiber was fused to the collimator with an embedded isolator in each channel to prevent backscattering light and send the laser beam into free-space.

By adjusting the half wavelength plates (HWPs), the four laser beams were combined by the polarization beam combiners (PBCs). M_1 and M_2 represent the all-reflectance and high-reflectance mirrors, respectively. After M_2, a little part of the beam was sent to a homemade pinhole with a 50-μm radius through a polarizer, and a photo detector laws placed immediately behind the pinhole. Another part of the beam after the splitter was sent to an infrared camera, which was used to profile the combined beam. The photo detector used was an InGaAs detector with a 700–1 800-nm response wavelength and 8.5-MHz bandwidth at a gain of 10 dB. The voltage signal was transformed by the photo detector, which was used to generate the phase control signal in the homemade signal processor (CM) based on the field programmable gate array (FPGA). The FPGA was programmed with the single-frequency dithering algorithm[13].

The principle of CPBC of multi-channel laser beams can be illustrated simply as follows. When the phase between two orthogonally polarized beams is undefined and injected into a PBC, the polarization state of the combined beam is uncertain and cannot be manipulated further (Fig. 2(a)). However, when the phase difference between the two orthogonal polarizations is locked and set to $\delta = n\pi$ (where n is an integer and δ is the phase difference between two beams), the polarization of the combined beam is pure linear-polarized (Fig. 2(b)), which can be combined again with a linearly polarized beam; thus, multi-channel beams can be combined through phase-locking.

The output power values obtained from the isolators of the 4 channels of fiber amplifiers are 1.2, 1.2, 1.1 and 0.9 W, respectively. When the system is in the open loop, the intensity profile at the camera is unstable due to the phase fluctuation in each channel. When the single-frequency dithering algorithm is implemented and the whole system is in the closed loop, the intensity profile at the camera is clear and steady. The combined output power measured at the output port of M_2 is 4.2 W. The combining efficiency is calculated to be 95%, where the combining efficiency (η) defined by the formula $\eta = P_{\mathrm{out}}/P_{\mathrm{in}}$, P_{out} is the combined output power, and P_{in} represents the total power after the collimators, which is measured to be 4.4 W.

The fidelity of CPBC and the phase noise suppression can be studied further using the time series signal and spectral density of energy collected by the pinhole of the PD (Fig. 3). When the system is in the open loop, the normalized energy is collected by the pinhole fluctuates randomly, whereas the normalized power in the pinhole can be locked effectively while the control module operates (Fig. 4). When the system is in the closed loop, the spectral density is about 30-dB lower than that in the open loop (Fig. 3), denoting an obvious compensation of the phase noise and a remarkable increase in coherent

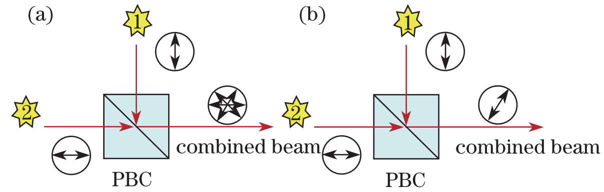

Fig. 2. Polarization states of two combined beams. (a) Random phase and (b) phase locked.

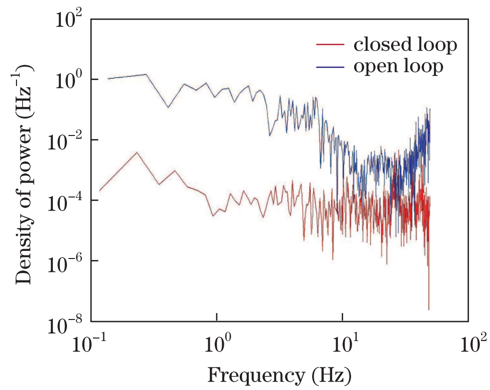

Fig. 3. Spectral density of energy in the pinhole in open loop and closed loop.

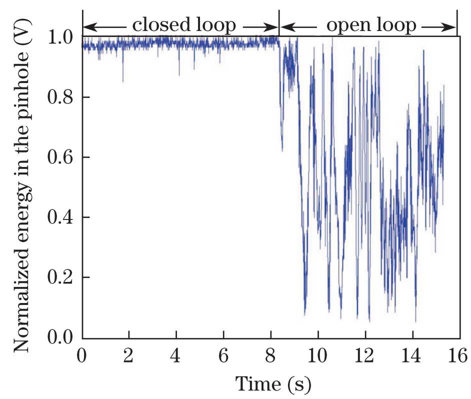

Fig. 4. Time series signals encircled in the pinhole in open loop and closed loop.

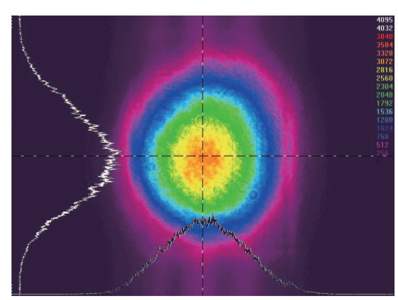

Fig. 5. 2D far-field images of the output produced by coherent combination of four beams.

combined output power. Figure 5 shows two-dimensional (2D) images of the four-beam combination result, which are similar to the profiles of the output of a single amplifier and can be characterized by the M^2 of approximately 1.1. Through measurement by a polarization extinction ratio meter (Thorlabs ERM100), the extinction ratio of the coherent polarization combined beam is more than 13 dB (95%), indicating that the output beam is nearly linear-polarized and can be further combined with another linear-polarized beam.

In the practical experimental system, such factors as overlap error (i.e., the beams cannot be superposed entirely due to the precision of the mechanical tuning devices), tilt error (i.e., the laser beams cannot be exactly coaxial due to the precision optical machining and assembling) and phase error (i.e., phase differences between beams due to the performance of phase compensating system), influence the combining efficiency of the CPBC system. High precision adjustment with micron-level accuracy can alleviate the influence of overlap error and tilt error. The influence of phase error can be improved by enhancing the precision of photo-detector, boosting the control band of the single-frequency dithering technique, and suppressing the noise of the phase-locking circuit.

In conclusion, we present CPBC of four polarization-maintained fiber amplifiers based on single-frequency dithering technique. The combining efficiency of the whole system can be as high as 95% when the system is in closed loop. Moreover, according to the time series signal and spectral density of energy collected by the pinhole, the phase noise is suppressed effectively. We believe that the CPBC scheme can be extended to multi-channels and has the potential in scaling high power with excellent beam quality.

References

1. Y. Xue, B. He, J. Zhou, Z. Li, Y. Yuan, F. Qi, C. Liu, J. Yuan, B. Zhang, and H. Lou, Chin. Phys. Lett. **28,** 054212 (2011).
2. Y. Jeong, J. Nilsson, J. K. Sahu, D. N. Payne, R. Horley, L. M. B. Hickey, and P. W. Turner, IEEE J. Sel. Top. Quantum Electron. **13,** 546 (2007).
3. C. J. Corcoran and F. Durville, Appl. Phys. Lett. **86,** 201118 (2005).
4. G. D. Goodno, C. P. Asman, J. Anderegg, S. Brosnan, E. C. Cheung, D. Hammons, H. Injeyan, H. Komine, W. H. Long, Jr., M. McClellan, S. J. McNaught, S. Redmond, R. Simpson, J. Sollee, M.Weber, S. B.Weiss, and M. Wickham, IEEE J. Sel. Top. Quantum Electron. **13,** 460 (2007).
5. J. Bourderionnet, C. Bellanger, J. Primot, and A. Brignon, Opt. Express **19,** 17053 (2011).
6. M. A. Vorontsov, T. Weyrauch, and L. A. Beresnev, IEEE J. Sel. Top. Quantum Electron. **15,** 269 (2009).
7. C. X. Yu, S. J. Augst, S. M. Redmond, K. C. Goldizen, D. V. Murphy, A. Sanchez, and Y. Y. Fan, Opt. Lett. **36,** 2686 (2011).
8. J. Li, K. Duan, Y. Wang, W. Zhao, J. Zhu, and Y. Guo, IEEE Photon. Technol. Lett. **20,** 888 (2008).
9. S. J. Augst, J. Ranka, T. Y. Fan, and A. Sanchez, J. Opt. Soc. Am. B **24,** 1707 (2007).
10. V. Jolivet, P. Bourdon, B. Bennaï, L. Lombard, D. Goular, E. Pourtal, G. Canat, Y. Jaouën, B. Moreau, and O. Vasseur, IEEE J. Sel. Top. Quantum Electron. **15,** 257 (2009).
11. X. Fan, J. Liu, and J. Wu, Chin. Opt. Lett. **8,** 48 (2010).
12. X. Li, X. Dong, H. Xiao, X. Wang, and X. Xu, Chin. Opt. Lett. **9,** 101401 (2011).
13. Y. Ma, X. Wang, J. Leng , H. Xiao, X. Dong, J. Zhu, W. Du, P. Zhou, X. Xu, L. Si, Z. Liu, and Y. Zhao, Opt. Lett. **36,** 951(2011).
14. P. Zhou, X. Wang, Y. Ma, H. Ma, X. Xu, and Z. Liu, Laser & Optoelectronics Progress (in Chinese) **47,** 021401 (2009).
15. R. Uberna, A. Bratcher, and B. G. Tiemann, IEEE J. Quantum Electron. **46,** 1191 (2010).
16. R. Uberna, A. Bratcher, and B. G. Tiemann, Appl. Opt. **49,** 6762 (2010).
17. S. H. Xu, Z. M. Yang, T. Liu, W. N. Zhang, Z. M. Feng, Q. Y. Zhang, and Z. H. Jiang, Opt. Express **18,** 1249 (2010).